ACS APPLIED MATERIALS & INTERFACES

Research Article

www.acsami.org

Updating Biomass into Functional Carbon Material in Ionothermal Manner

Pengfei Zhang,[†,‡] Yutong Gong,[†] Zhongzhe Wei,[†] Jing Wang,[†] Zhiyong Zhang,[‡] Haoran Li,[†] Sheng Dai,[‡] and Yong Wang*[,†]

[†]Carbon Nano Materials Group, Center for Chemistry of High-Performance and Novel Materials, Department of Chemistry, Zhejiang University, Hangzhou 310028, People's Republic of China

[‡]Chemical Science Division, Oak Ridge National Laboratory, Oak Ridge, Tennessee 37831, United States

Supporting Information

ABSTRACT: The development of meaningful ways to transfer biomass into useful materials, more efficient energy carriers, and/or carbon storage deposits is a profound challenge of our days. Herein, an ionothermal carbonization (ITC) method, via treating natural resources (glucose, cellulose, and sugar cane bagesse) in nonmetal ionic liquids (ILs) at ~200 °C, is established for the fabrication of porous heteroatom-doped carbon materials with high yield. Commercial ILs with bulky bis(trifluoromethylsulfonyl)imide anion or cross-linkable nitrile group were found to be efficient and recyclable templates for porosity control, leading to exciting nanoarchitectures with promising performance in oxygen reduction reaction. The optimized ILs (12 mL) can dissolve and directly convert up to 15 g of glucose into porous carbon materials (S_{BET}: 272 m^2/g) one time. This ITC method relies on the synergistic use of structure-directing effect, good biomass solubility, and excellent thermal stability of ILs, and provides a sustainable strategy for exploiting biomass.

KEYWORDS: *porous carbon, nitrogen-doped carbon, biomass, ionothermal synthesis, soft template, ionic liquid*

1. INTRODUCTION

The rapidly developing global economy has triggered excessive consumption of fossil fuels, posing significant threats to the society. A sustainable future for the functional materials requires feedstocks based on renewable rather than steadily depleting sources. In material community, porous carbon materials are raising more and more interest, due to their extraordinary chemical, mechanical, and thermal stability, wide abundance, and extensive applications.[1−3] Recently, heteroatom-doped (e.g., N, B, F, S) carbon materials have become a subject of great interest to chemists, as the incorporation of heteroatom can be considered as a tool for the tuning of carbon properties, at the same time affording carbon material with attractive feature for more tasks, such as electrodes in fuel cell and supercapacitor, CO_2 capture, etc.[4−6] To date, a large part of carbon materials are constructed from fossil fuel sources under relatively harsh conditions (e.g., direct pyrolysis of organic compounds, chemical vapor deposition, laser ablation), and therefore accessibility and sustainability of those procedures are somewhat limited.[7−11] In fact, excluding activated carbons, only a few investigations have been done to synthesize and recognize the structure of carbon materials based on natural resources.[12−14] To this end, a hydrothermal carbonization (HTC) process has been well studied in the past decade, which allows the transformation of biomass into carbonaceous products.[16−19] For example, carbon materials based on microalgae, a fast-growing biomass, have been recently prepared by the HTC process; nonetheless, those materials are essentially nonporous (S_{BET} ≈ 6 m^2/g), as usually observed for HTC carbon materials.[20] The nonporous nature of those carbons from direct HTC method largely limited their applications, although hard templates, soft templates, and some other efficient additives have been recently coupled with HTC technique for porosity control.[16,18,19,21,22] Until recently, one-step methodology for the preparation of porous carbons, in particular carbons with specific foreign atoms, from renewable precursors is still highly welcomed.

Initially developed as molten electrolytes for battery applications, already ionic liquids (ILs) have impacted various fields beyond their originally designed conception, such as catalysis, chemical synthesis, CO_2 capture, and material science.[23−31] In the field of carbon material, a straightforward approach to nitrogen-rich porous carbons via pyrolysis of ILs with cross-linkable cations or anions has been recently unveiled.[32−34] This self-templated process did not need any other scaffolds or additives, and the porosity could be controlled by the size of anions in the ILs. However, their way toward practical application is obstructed by the high price

Received: April 22, 2014
Accepted: July 8, 2014
Published: July 8, 2014

of those ILs. In addition, recent works indicated that ILs are also active in solubilizing biomass; for instance, commercial 1-butyl-3-methylimidazolium chloride ([Bmim]Cl) can effectively break the extensive hydrogen-bonding network present, thus allowing for dissolution of more cellulose than the traditional solvent systems.[35−37] Inspired by the versatility of ILs, structure-directing ability, unique feature on dissolving biomass, excellent thermal stability, and negligible vapor pressure, we ask if ILs can work as recyclable templates and solvents for the transformation of renewable biomass into porous carbons in an ionothermal manner. As an analogue of hydrothermal and solvothermal approaches, ionothermal synthesis, that is, reaction conducted in ILs, is widely used for the preparation of metal nanoparticles (e.g., Ru, Pd, Ir, etc.), inorganic solids (e.g., zeolite, TiO_2, SiO_2, etc.), or organic−inorganic hybrid materials (e.g., metal organic frameworks) with unprecedented structures and properties, yet seldom seen in carbon construction.[38−43] A more recent work presented iron-containing ILs ([Bmim][$FeCl_4$]) as ionothermal solvent for the conversion of carbohydrate precursors into porous carbon materials, in which the porosity was actually induced by the iron species because the [Bmim][Cl] alone could only lead to nonporous carbonaceous materials.[42]

In this contribution, we wish to show the rational application of metal-free ILs as "recyclable templates" in the ionothermal carbonization (ITC) of glucose, cellulose, and industry waste-sugar cane bagasse into nanostructured carbon materials with controllable surface area, morphology, and composition. Those versatile ILs were believed to function as templates, solvents, and heteroatom sources in the ionothermal process. Depending on the ILs nature, micro- to mesoporous materials with specific surface areas up to 627 m^2/g are directly obtained from biomass, without any activation process while preserving the targeted chemical functionality.

2. EXPERIMENTAL SECTION

2.1. Chemicals. All of the ionic liquids were purchased from J&K Chemicals. D-Glucose (99%) and α-cellulose (particle size <25 μm) were obtained from Aladdin Chemistry Co., Ltd. Fresh sugar cane was collected from Guangxi (China). All of the chemicals were used without further treatment.

2.2. Characterization Method. N_2 sorption analysis was performed at 77 K using a TRISTAR II3020 instrument, equipped with automated surface area and pore size analyzer. Before analysis, samples were degassed at 150 °C for 20 h using a masterprep degassing system. The carbon morphology was visualized using a Gemini scanning electron microscope (SEM). Transmission electron microscopy (TEM) was carried out with a HT-7700 instrument. Elemental analysis was obtained on an EA 1112 elemental analyzer (ThermoFinnigan Italia S. P. A). The X-ray photoelectron spectra (XPS) were obtained with an ESCALAB MARK II spherical analyzer using a magnesium anode (Mg 1253.6 eV) X-ray source. The powdered samples were pressed to pellets and fixed to a stainless steel sample holder without further treatment. The XPS spectrum was shifted according to C 1s peak being at 284.6 eV, so as to correct the charging effect. Thermal gravimetric analysis (TGA) was performed on TGA 7 from Perkin Elmer. The online FT-IR spectra were recorded on a Bruker MATRIX-MF.

2.3. Synthesis of ITC Carbon in Closed Autoclave. *2.3.1. Synthesis of ITC Carbon from Glucose.* In a typical synthesis, 2 g of glucose was dissolved in 10 mL ILs, and then the mixture was loaded into a PTFE-lined autoclave. As 2 g of glucose cannot be dissolved in hydrophobic IL-d (8 mL) only, hydrophilic and highly polar IL-e (4 mL) was introduced to completely dissolve glucose, in the case of IL-d. After treatment at 200 °C for 24 h, the resulting mixture was thoroughly washed in 200 mL of ethanol, and then brown or black solid was obtained by filtration. The final products were obtained by freeze-drying. The filtrate then could be concentrated under reduced pressure, affording recovered ILs. Part of those materials were further postcarbonized at 600 °C (heating rate, 2.5 K/min; holding time, 4 h) or 900 °C (heating rate, 3.75 K/min; holding time, 1 h) under an inert N_2 atmosphere (N_2 500 mL/min). After being cooled to room temperature, black carbon materials were obtained. Those carbon materials were denoted as G-ILa@200, etc., where the second word corresponds to the used IL while the last number "200" means the final treated temperature (G: glucose).

2.3.2. Synthesis of ITC Carbon from Cellulose. In a typical synthesis, 2 g of cellulose was dissolved in 14 mL of IL-e with ∼40 μL of deionized water as additive, and then the mixture was loaded into a PTFE-lined autoclave. After treatment at 200 °C for 24 h, the resulting mixture was treated as described in the above section. Those carbon materials were denoted as C-ILe@200, etc. (C: cellulose).

2.3.3. Synthesis of ITC Carbon from Sugar Cane Bagasse. The sugar cane was chewed for ∼5 min and then thoroughly washed with deionized water at 80 °C for 12 h, to remove residual soluble sugars. The raw sugar cane bagasse was dried at 70 °C overnight and milled to a size less than 0.5 cm. It is composed of 44.7% cellulose, 27.2% hemicellulose, 19.7% lignin, 1.1% ash, and 7.3% other components. In a typical synthesis, 0.5 g of bagasse was added into 10 mL of IL-e with ∼40 μL of deionized water, and then the mixture was loaded into a PTFE-lined autoclave. After treatment at 200 °C for 24 h, the resulting mixture was thoroughly washed with ethanol, and then black solid was obtained by centrifugation. The final product was obtained by freeze-drying, labeled by B-ILe@200.

2.4. Electrochemical Measurement for Oxygen Reduction Reaction. The oxygen reduction reaction performance of the fabricated carbon materials was measured using a traditional three-electrode system. A glassy carbon electrode (d = 3 mm) was applied as working disk for CV, and a rotating disk electrode (d = 5 mm, Pine, CPR) was used for linear sweep voltammograms (LSV). The data were collected using a LK-2005A electrochemical workstation. The reference electrode was a SCE electrode, and the counter electrode was platinum foil.

The working electrode was prepared as follows: 10 mg of catalyst, 50 μL of Nafion aqueous solution (5%), and 500 μL of ethanol were mixed and ultrasonically dispersed into a uniform suspension. 2.5 μL of the ink was then dropped onto the glassy carbon and 5 μL for the rotating disk electrode via a microsyringe, which yielded a loading of catalyst = 0.643 and 0.463 mg/cm^2, respectively. The CV and LSV curves then were recorded in 0.1 M KOH aqueous solution.

3. RESULTS AND DISCUSSION

3.1. Ionothermal Carbonization of Glucose. The work presented herein focuses on the design, control, and mechanism analysis of ionothermal synthesis for carbon construction from biomass or its derivates. Scheme 1 shows the chemical structures of representative ILs for ionothermal process. Glucose, a common sugar, was selected as model substrate to investigate the ITC processes under different

Scheme 1. Chemical Structures of Ionic Liquids for Ionothermal Carbonization

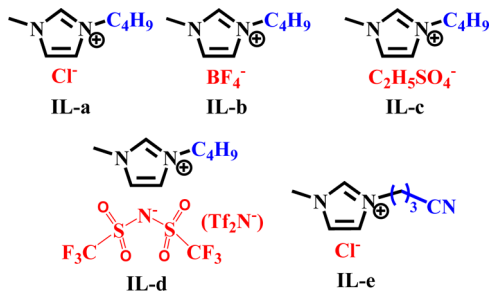

conditions. In general, ITC of glucose was carried out at 200 °C for 24 h by dissolving 2 g of glucose in 10 mL of ILs, and a part of the ITC carbon material (after the removal of ILs by washing in ethanol) was further carbonized to 600 or 900 °C under an inert N_2 atmosphere to yield a carbon material with higher carbon content. Those carbon materials were denoted as G-ILa@200, etc., where the second word corresponds to the used IL while the last number "200" means the final treated temperature (G, glucose; C, cellulose; B, bagasse).

SEM images show various morphologies of the ITC carbon materials, from irregular and bulky agglomerates to porous nanostructures, determined by the nature of ILs (Figure 1, Supporting Information Figure S1). Interestingly, the anion of ILs affected the ITC process so much. The use of IL-d with big $[Tf_2N^-]$ resulted in nanostructured material, composed of agglomerated nanoparticles generating a high degree of interstitial porosity (Figure 1d), while the IL-c with relatively smaller anion ($C_2H_5SO_4^-$) afforded less porous carbon (Figure 1c). In sharp contrast, nonporous bulky materials with microparticles or lumps (>10 μm) were obtained in the presence of ILs with small BF_4^- or Cl^- anions (Figure 1a,b, Supporting Information Figure S2). Those results suggest that ILs with large anions are exactly in favor of porosity formation, certainly upon the promise of nice sugar solubility. When nitrile-containing [BCNmim]Cl (IL-e) was used in place of common [Bmim]Cl (IL-a), significant changes occurred in ITC process, thereby giving product with sponge-like carbonaceous nanoarchitecture that comprises spherically shaped particles around ~60 nm (Figure 1e,f). It should be noted that carbon nanoparticles (<100 nm) prepared with this ITC strategy are distinctly smaller than those (>1 μm) in the hydrothermal carbonization of glucose (Supporting Information Figure S3).

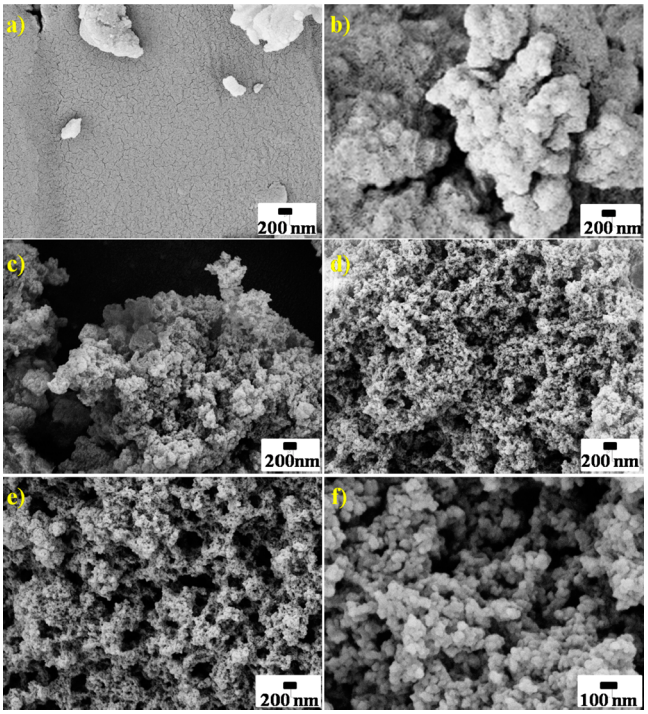

Figure 1. SEM images of different ionothermal carbon materials: (a) G-ILa@200, (b) G-ILb@200, (c) G-ILc@200, (d) G-ILd@200, and (e,f) G-ILe@200.

TEM images further reveal the hierarchical nanomorphology of ITC carbons (Supporting Information Figure S4).

The porosity of the ITC carbons was determined using N_2 sorption analysis at 77 K (Table 1, Figure 2). The samples with large lumps or microspheres (G-ILa@200 and G-ILb@200) showed low BET surface areas, while N_2 isotherms of G-ILd@200 and G-ILe@200 indicated relatively high BET surface areas (up to 117 m^2/g), additional straightforward evidence for the efficiency of this "IL templating" method with IL-d or IL-e as solvent. After postcarbonization treatment, BET surface areas of as-synthesized carbons (e.g., G-ILd@600) could be further enhanced to ~499 m^2/g, as a result of microporosity development upon thermal treatment related to the elimination of organic groups and gases.[44] Pore size distribution profiles for as-made materials located in a broad range, covering both micropores and mesopores (Supporting Information Figure S5).

As shown in Table 1, product yields of the ITC of glucose (45−75 wt %) were a little higher than the corresponding HTC of glucose (32 wt %, Supporting Information Figure S3), and thermal treatment at 600−900 °C would further lower the yields, possibly due to a rearrangement process with the loss of CO, CO_2, and CH_4.[44] Table 1 also shows the elemental chemical composition of ITC materials. As compared to pure glucose (C: 40.0 wt %), we observed a significant increase in carbon content after ionothermal treatment, confirming its "carbonization effect". More specifically, carbon contents of ITC carbons vary from 51.1 to 63.7 wt %. Further analysis suggests that the evolution of elemental compositions from the raw material to the ITC material basically follows the trend corresponding to a dehydration process, similar to that previously observed in the HTC transformation of saccharides.[44] It is worth mentioning that once the autoclave has cooled, there was only a slight overpressure inside the vessel (~0.2 MPa). We interpret that during this ITC process, the decarboxylation-induced gaseous products (e.g., CO_2 and CO) generate in a small amount, around 12 mol % based on carbon in the glucose, which was estimated via the gas left inside the autoclave by the Ideal Gas Law ($PV = nRT$).

In addition, elemental analysis demonstrates the nitrogen-doped character of some carbons prepared in this ITC method (N: 3.6−8.0 wt %); for example, the amount of nitrogen is as high as 6% in the porous G-ILe@200 sample. Fluorine and boron heteroatom can also be flexibly introduced into ITC carbon framework by selecting $[Bmim][BF_4]$ (IL-b) as solvent, and XPS measurement of G-ILb@600 sample afforded the corresponding F 1s binding energy (BE) peak (ca. 685.7 eV) and B 1s BE peak (ca. 191.7 eV) (Figure 2c,d). It is not surprising because the IL solvents are often incorporated into the final products in the ionothermal synthesis of zeolite.[45] In fact, the amount of ILs participating in the ITC process is relatively low; for example, based on elemental analysis, only ~2.6% IL-e took part in the cross-polymerization reaction, given that all of the nitrogen atoms in ILs fell into the ITC products.

After further carbonization, the carbon content increased to ~90% (G-ILd@900:89.8%), while nitrogen content stayed virtually constant, revealing that those nitrogen atoms can actually be incorporated in the aromatization/pseudographitization process of the carbon structure. High-resolution N 1s XPS analysis of G-ILd@900 showed the presence of quaternary-type (401.2 eV: 53.2%), pyridinic- (398.6 eV: 37.0%), and pyrrolic- (399.9 eV: 9.8%) nitrogen environments,

Table 1. Characterization of ITC and Thermal Treated Carbon Materials[a]

sample	yield (%)	C (%)	N (%)	S_{BET} (m^2/g)	V_{pore} ($cm^3\ g^{-1}$)	V_{meso} ($cm^3\ g^{-1}$)
G-ILa@200	46	59.0	ADL	<10		
G-ILb@200	75	51.1	8.0	<10		
G-ILc@200	45	60.3	ADL	16	0.08	0.04
G-ILd@200	53	59.7	4.8	117	0.28	0.22
G-ILd@200-L	55	63.7	2.8	272	0.44	0.34
G-ILe@200	50	61.1	6.0	36	0.12	0.07
G-ILe@200-L	52	63.3	5.1	99	0.16	0.14
G-ILd@600	30	79.0	4.8	499	0.43	0.20
G-ILd@600-L	32	82.8	3.4	442	0.56	0.32
G-ILe@600	25	80.0	5.0	321	0.21	0.06
G-ILe@600-L	33	81.5	3.9	627	0.53	0.42
G-ILd@900	26	89.8	3.6	221	0.23	0.14
G-ILe@900	27	91.4	4.8	445	0.48	0.23
C-ILe@200	62	51.4	3.2	73	0.16	0.05
C-ILe@600	24	80.7	4.4	365	0.23	0.04
B-ILe@200	37	44.0	6.6	35	0.15	0.11
B-ILe@600	18	76.7	5.8	320	0.51	0.27

[a]Yields were based on the weight ratio between products and carbon precursors. S_{BET}: Brunauer–Emmett–Teller (BET) surface area. V_{pore}: Total pore volume calculated at P/P_o = ~0.99. V_{meso}: Mesoporous volume from BJH method and N_2 adsorption data for pore diameters between 2 and 50 nm. ADL: At detection limit.

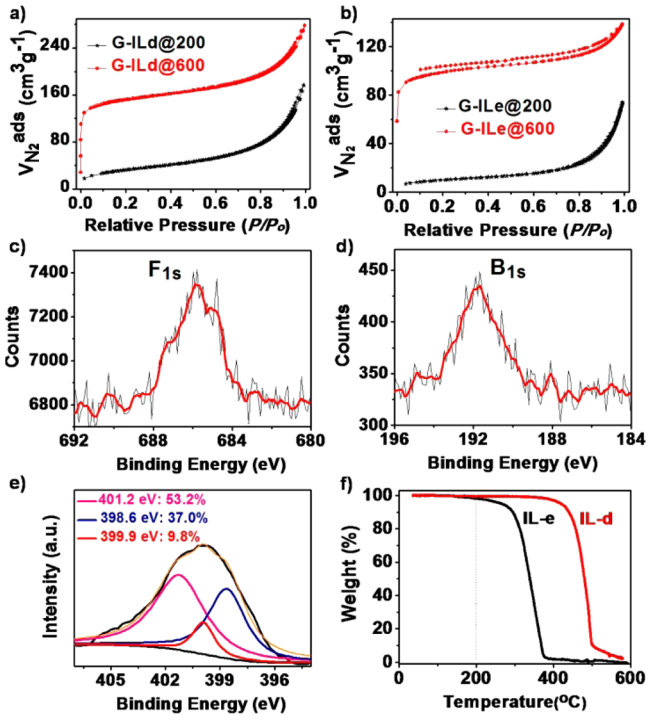

Figure 2. (a,b) N_2 isotherm curves for ionothermal carbons and as-synthesized carbons by postcarbonization, (c,d) XPS spectra of G-ILb@600 sample, (e) N 1s XPS spectra for G-ILd@900 sample, and (f) TGA curves of ionic liquids in N_2 atmosphere.

suggesting the successful doping of nitrogen into the aromatic carbon matrix, with the quaternary-type system dominating (Figure 2e).

We then moved toward the recycling ability of ILs. IL-d and IL-e, serving as porogens in the HTC process, here were studied as examples. Evidence from the thermal gravimetric analysis (TGA) profiles for IL-d and IL-e confirms their good thermal stability at ITC temperature (200 °C), providing a great prerequisite for recovering ILs (Figure 2f). Simply, after the ITC of glucose with fresh ILs, those used ILs were recovered by ethanol extraction and concentration. The ILs solvent could be used at least four times without losing their structure-directing role, as suggested by the S_{BET} surface area and morphology of products (Supporting Information Table S1). For instance, SEM pictures of ITC carbons from recovered ILs clearly show continuous porous nanostructures, consisting of <100 nm sized particles, a typical morphology of ITC carbons (Supporting Information Figure S6). It should be mentioned that full recovery of ILs is impossible, because a small part of ILs took part in the ITC process. The average recovery of ILs in four cycles was around 90% (Supporting Information Table S1).

Another key point related to the ITC method for practical application is its capacity of converting substrate, and we would then probe the maximum glucose amount that a certain amount of ILs can convert one time. Initially, dissolution experiments were carried out in ILs mixture, and glucose was gradually added into the solvent under stirring (Figure 3a). We noticed that the ILs mixture (12 mL: IL-d, 8 mL; IL-e, 4 mL) can dissolve up to 15 g of glucose, and a brown, viscous solution was obtained (Figure 3b). To our delight, 8.2 g of ITC carbon product (G-ILd@200-L; yield: ~55%) was obtained, and the carbon content can reach 63.7%, thus arguing for the successful dehydration of glucose. In addition, N_2 sorption measurement performed on G-ILd@200-L showed a satisfying BET surface area of 272 m^2/g (Figure 3c). One can observe that the achieved surface area can be listed as one of the highest values for low temperature (≤250 °C) carbonization of biomass (Supporting Information Table S2). As to the corresponding sample thermally treated at 600 °C (G-ILd@600-L), a leap in N_2 uptake was observed, and its BET surface area came to 442 m^2/g. Complementary TEM image of G-ILd@200-L sample shows a hierarchical matrix comprising interconnected particles (Figure 3d). Indeed, the present synthesis functions well for more than 7-fold glucose substrate with the same amount of ILs. The polar IL-e was also studied in high glucose concentration, and it (10 mL) can dissolve a maximum 12 g of glucose, as shown in Figure 3f. The corresponding ITC

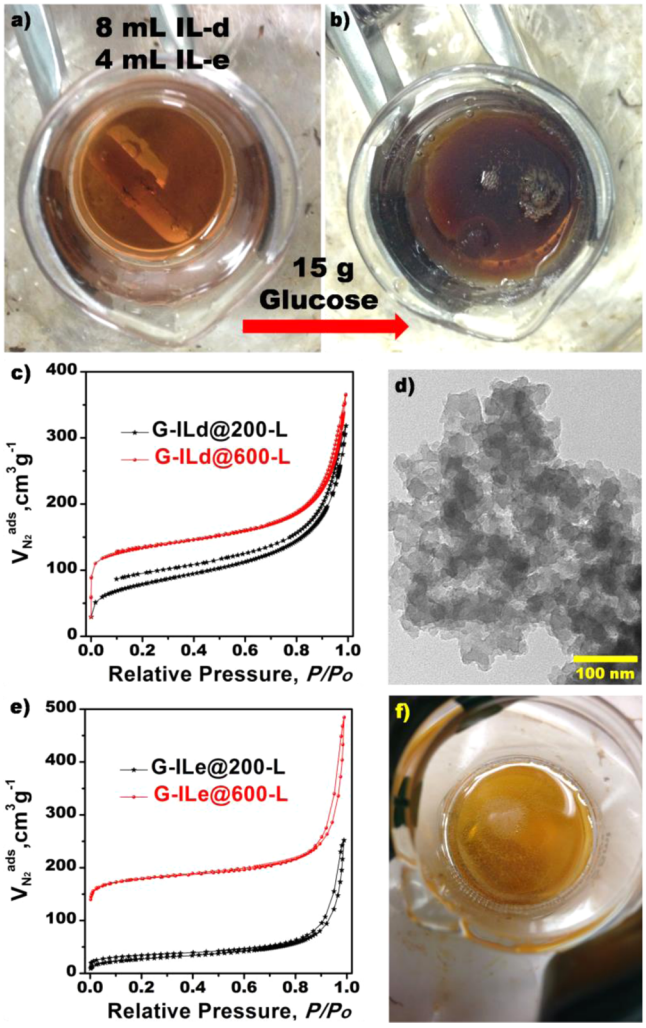

Figure 3. (a) A mixture of ILs in 200 °C oil bath, (b) viscous solution of ILs–glucose mixture, (c) N_2 sorption curves of ITC carbons prepared in large scale, (d) TEM picture of G-ILd@200-L sample, (e) N_2 sorption curves of ITC carbons prepared in IL-e, and (f) viscous solution of ILs–glucose mixture: IL-e 10 mL and glucose 12 g.

carbon from IL-e held a BET surface area of 99 m^2/g, and further thermal treatment could enhance it to 627 m^2/g (Figure 3e).

3.2. Ionothermal Carbonization of Cellulose and Sugar Cane Bagasse. As the most abundant and inexpensive saccharide, cellulose is one of the most potential materials, available for nanoporous carbon production.[18,46] In subsequent investigation, we tried to carry out the ITC of cellulose with IL-e, the one with both satisfactory ability in directing porosity and good cellulose solubility.[35,36] After ITC of cellulose at 200 °C for 24 h, ultralight and monolithic carbon aerogel was presented (Figure 4a). The density of our C-ILe@200 sample (ρ = ~0.02 g/cm^3) is significantly lower than that of the reported highly porous aerocellulose (ρ = ~0.15 g/cm^3).[47] SEM and TEM pictures of this ITC product exhibit a continuous, hierarchically structured, nanometer-scale, and porous network, made up primarily from carbon nanospheres ranging between ~50 and 150 nm, which is totally different with the irregular morphology of pristine cellulose (Figure 4b,c, Supporting Information Figure S7). The extensive porosity of cellulose-derived carbon was then confirmed by N_2 (77 K) sorption tests, with BET surface area up to 365 m^2/g (Table 1, Figure 5a). Furthermore, the IL-e with nitrile group effectively introduced nitrogen atoms into ITC carbon (N: 3.2 wt %), as expected.

Another lignocellulosic waste, sugar cane bagasse, is an unexplored, yet potential resource with very low cost and wide availability, but it is indeed a notorious recalcitrant due to the highly lignified and crystalline structure (Figure 4d,e). Under the applied ITC conditions (200 °C, 24 h), mechanically hard sugar cane bagasse with interconnected sheet structure was essentially disintegrated, resulting in a nice dispersion of carbon aggregations with significantly reduced size (Supporting Information Figure S8). High-resolution SEM indicates the presence of a developed pore system with apparent pore sizes around 10–100 nm (Figure 4f). Porous carbon with BET surface area of 320 m^2/g can be obtained by simple thermal treatment of the ITC carbon from sugar cane bagasse (Figure 5a). Again, the nanoporous carbons turn out to be successfully

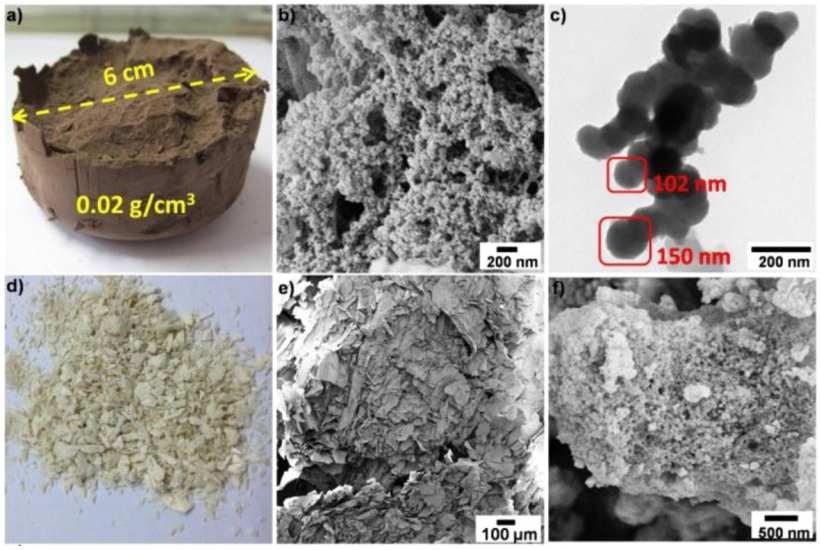

Figure 4. (a) Carbon aerogel from cellulose, (b,c) SEM and TEM pictures of C-ILe@200 sample, (d) sugar cane bagasse, (e) SEM image of sugar cane bagasse, and (f) SEM image of B-ILe@200 sample.

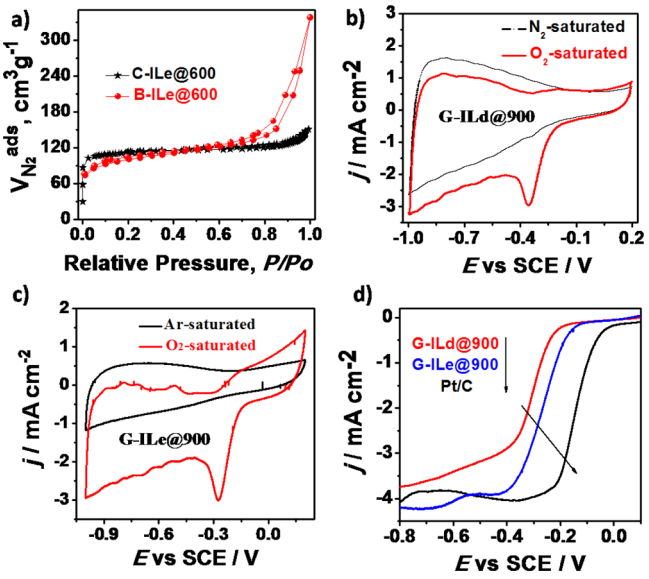

Figure 5. (a) N_2 isotherm curves for carbon materials from cellulose (C-ILe@600) and sugar cane bagasse (B-ILe@600), (b) cyclic voltammograms of G-ILd@900 in 0.1 M KOH, scan rate 50 mV/s, (c) cyclic voltammograms of G-ILe@900 in 0.1 M KOH, and (d) voltamperograms for oxygen reduction on different electrodes in O_2-saturated 0.1 M KOH at a certain rotation speed (900 rpm), scan rates 50 mV/s.

incorporated with nitrogen atoms, as indicated by elemental analysis (N: 5.8−6.6 wt %).

3.3. Electrochemistry Performance of ITC Carbon.

Recent examples show that heteroatom-doped carbon materials represent an interesting class of functional materials for numerous applications.[48] Our synthetic approach for fabricating porous carbons with tunable heteroatoms should pave the way for some refined electronic applications. The resulting nitrogen-doped products (e.g., G-ILd@900 and G-ILe@900) were, for instance, used as metal-free electrocatalyst for the oxygen reduction reaction (ORR) (Figure 5). Initially, the electrocatalytic activity of G-ILd@900 for ORR was examined by cyclic voltammetry (CV) in 0.1 M KOH solution saturated with nitrogen/argon or oxygen. As shown in Figure 5b, no obvious current response is observed within the potential range from −1.0 to +0.2 V in the N_2-saturated solution. In contrast, a well-defined cathodic peak around −0.35 V emerges when the electrolyte solution is saturated with O_2, suggesting a pronounced catalytic activity of G-ILd@900 for oxygen reduction. In the presence of G-ILe@900, the O_2 reduction peak occurred at about −0.27 V (Figure 5c). To gain further insight into the kinetics, the ORR process was studied by a rotating disk electrode. The onset potential of G-ILe@900 for the ORR (∼ −0.1 V) is higher than the value by G-ILd@900, which is probably due to the higher nitrogen content and surface area of G-ILe@900 (Figure 5d). So, this nitrogen-doped carbon from ITC process holds promising catalytic activity for ORR process. However, the ORR activity of as-made carbon material is still lower than that of the commercial Pt/C catalyst, respecting the onset potentials.

3.4. Mechanism Study of Ionothermal Carbonization.

As a general premise, stirring carbon precursors in ILs under ambient condition could lead to dissolution, although gently heating is necessary in some cases. Under current ITC conditions, glucose would basically follow a typical sugar decomposition route.[49] In the initial stage, glucose dehydrates to furfural-like compounds and then proceeds with further polymerization−polycondensation to a polyfuran network. Once supersaturated, polyfuran-type units precipitate from the homogeneous solution, and then grow into secondary spherical particles of the final size. The above-mentioned route is a general understanding of the ITC process. We would then concentrate on the reason why ionothermal synthesis can result in exciting porosity. The two IL porogens, IL-d with $[Tf_2N^-]$ and the nitrile-containing IL-e, are believed to function in different routes.

Controlled carbonization of glucose in the presence of $LiTf_2N$ under ionothermal or hydrothermal conditions led to carbon products without porosity (S_{BET} < 3 m^2/g), revealing the organic cation in IL is necessary for forming porosity (Supporting Information Note 1). Previous studies on the chemical structure of ILs suggested imidazolium cations can form extended hydrogen-bond interactions with up to three anions, affording highly structured IL clusters of minimal free

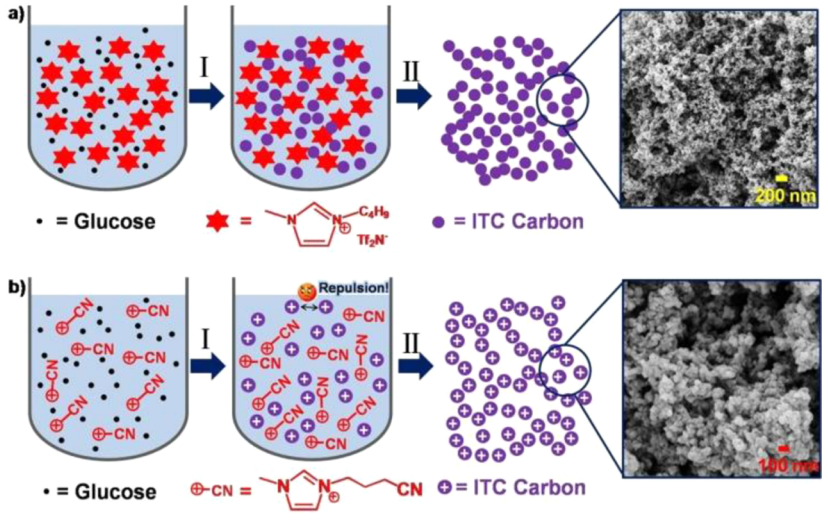

Figure 6. (a) ITC of glucose with IL-d as solvent, and (b) ITC of glucose with IL-e as solvent. (I) 200 °C, 24 h, in autoclave; (II) washing with ethanol.

energy,[49−52] and ILs are therefore "supermolecular" solvents.[39] Decidedly, the IL-d with bulky [Tf_2N^-] is expected to exist as much bigger IL clusters, in particularly comparing with IL-a with small [Cl^-]. In the presence of IL-d, the polymerization−polycondensation process of furfural-like monomer may proceed around the big IL clusters, and abundant interstitial pores appear after removal of the big "IL clusters template" (Figure 6a). Meanwhile, the IL clusters, inserted in those small carbon nuclei, could timely interrupt their growing process, resulting in carbon particles with decreased sizes.

It is well-known that the nitrile group in IL-e can undergo cross-linking reactions under appropriate conditions, a unique feature of IL-e that differs from other tested ILs.[32−34,53] In the ITC of glucose, the polymerization between monomers (e.g., HMF, furfural, and 5-methylfurfural) and nitrile group on the cation of IL-e may occur and afford primary carbon particle with positive charge (Figure 6b). The cross-polymerization is valid, because in the ITC of glucose, changing the IL-e ([BCNmim][Cl]) to IL-a ([Bmim][Cl]) leads to significant changes in nitrogen content of the products (6.0% vs <0.1%, respectively), and the transfer of nitrogen atoms from IL-e to ITC products is exactly bridged by the reaction between nitrile group of IL-e and those monomers from glucose. As mentioned in previous work, the strong electrostatic repulsion between particles can largely interrupt the interconnecting reactions (e.g., intermolecular dehydration and aldol condensation) and minimize their agglomeration, therefore attaining small carbon particles with extensive interstitial porosity.[21]

4. CONCLUSIONS

In summary, a facile, direct, and controllable ITC approach has been established to convert biomass into heteroatom-doped porous carbon materials. The morphology, porosity, and composition of the resulting carbon can be nicely controlled by the cation/anion pairing within the IL. Notably, the role of the ionothermal solvent is discussed in detail, and the two "IL porogens" ([Tf_2N^-] or nitrile containing ILs) are supposed to work through "big IL cluster templating" means and "electrostatic repulsion-induced molding" way, respectively.

Thanks to the designable ILs, diverse carbons, doped with B, F, or N atoms, can be simply fabricated by the versatile ITC strategy, with exciting opportunities for many specific applications. Assisted by the good biomass solubility of specific ILs, the current ITC method can be extended for the upgrading of cellulose and sugar cane bagasse into high value carbon materials with attractive features. We expect that the ITC manner will provide an effective platform for exploiting biomass. It should be mentioned that the ILs solvent can be easily recovered and reused at least three times with similar functions, arguing for its satisfying sustainability.

The ionothermal synthesis has been unveiled around one decade, but its unexpected talent for carbon material is a young topic, yet full of promise. For example, the evolution of glucose in carbonization could be studied by in situ FTIR test under ionothermal system (Supporting Information Figure S9). We believe that a number of carbon precursors can be polymerized in controlled ITC manners, affording much more advanced carbon materials with unique structures in the near future.

■ ASSOCIATED CONTENT

Supporting Information

More SEM and TEM images, mechanism study, and a brief summary of HTC/ITC materials: Figures S1−9, Tables S1,2, and Note S1. This material is available free of charge via the Internet at http://pubs.acs.org.

■ AUTHOR INFORMATION

Corresponding Author

*E-mail: chemwy@zju.edu.cn.

Notes

The authors declare no competing financial interest.

■ ACKNOWLEDGMENTS

Financial support from the National Natural Science Foundation of China (21376208 and U1162124), the Zhejiang Provincial Natural Science Foundation for Distinguished Young Scholars of China (LR13B030001), the Specialized Research Fund for the Doctoral Program of Higher Education (J20130060), the Fundamental Research Funds for the Central Universities, the Program for Zhejiang Leading Team of S&T Innovation, the Partner Group Program of the Zhejiang University, and the Max-Planck Society is greatly appreciated. P. Zhang and S. Dai. were supported as part of the Fluid Interface Reactions, Structures and Transport (FIRST) Center, an Energy Frontier Research Center funded by the U.S. Department of Energy, Office of Science, Office of Basic Energy Sciences under Award Number ERKCC61.

■ REFERENCES

(1) Antonietti, M.; Müllen, K. Carbon: The Sixth Element. *Adv. Mater.* **2010**, *22*, 787.

(2) Liang, C.; Li, Z.; Dai, S. Mesoporous Carbon Materials: Synthesis and Modification. *Angew. Chem., Int. Ed.* **2008**, *47*, 3696−3717.

(3) Liang, H.; Guan, Q.; Chen, L.; Zhu, Z.; Zhang, W.; Yu, S.-H. Macroscopic-Scale Template Synthesis of Robust Carbonaceous Nanofiber Hydrogels and Aerogels and Their Applications. *Angew. Chem., Int. Ed.* **2012**, *51*, 5101−5105.

(4) Wei, J.; Zhou, D.; Sun, Z.; Deng, Y.; Xia, Y.; Zhao, D. Y. A Controllable Synthesis of Rich Nitrogen-Doped Ordered Mesoporous Carbon for CO_2 Capture and Supercapacitors. *Adv. Funct. Mater.* **2013**, *23*, 2322−2328.

(5) Guo, D.; Mi, J.; Hao, G.; Dong, W.; Xiong, G.; Li, W.; Lu, A.-H. Ionic Liquid $C_{16}mimBF_4$ Assisted Synthesis of Poly(benzoxazine-co-resol)-based Hierarchically Porous Carbons with Superior Performance in Supercapacitors. *Energy Environ. Sci.* **2013**, *6*, 652−659.

(6) Vinu, A.; Terrones, M.; Golberg, D.; Hishita, S.; Ariga, K.; Mori, T. Synthesis of Mesoporous BN and BCN Exhibiting Large Surface Areas via Templating Method. *Chem. Mater.* **2005**, *17*, 5887−5890.

(7) Wang, D.; Li, F.; Liu, M.; Lu, G. Q.; Cheng, H.-M. 3D Aperiodic Hierarchical Porous Graphitic Carbon Material for High-Rate Electrochemical Capacitive Energy Storage. *Angew. Chem., Int. Ed.* **2008**, *47*, 373−376.

(8) Joo, S.; Choi, S.; Oh, I.; Kwak, J.; Liu, Z.; Terasaki, O.; Ryoo, R. Ordered Nanoporous Arrays of Carbon Supporting High Dispersions of Platinum Nanoparticles. *Nature* **2001**, *412*, 169−172.

(9) Zheng, Y.; Liu, J.; Liang, J.; Jaroniec, M.; Qiao, S. Z. Graphitic Carbon Nitride Materials: Controllable Synthesis and Applications in Fuel Cells and Photocatalysis. *Energy Environ. Sci.* **2012**, *5*, 6717−6731.

(10) Guo, T.; Nikolaev, P.; Rinzler, A.; TomBnek, D.; Colbert, D.; Smalley, R. Self-Assembly of Tubular Fullerenes. *J. Phys. Chem.* **1995**, *99*, 10694−10697.

(11) Eftekhari, A.; Jafarkhani, P.; Moztarzadeh, F. High-yield Synthesis of Carbon Nanotubes Using a Water-soluble Catalyst Support in Catalytic Chemical Vapor Deposition. *Carbon* **2006**, *44*, 1343−1345.

(12) Bansal, R. C.; Donnet, J. B.; Stoeckli, F. *Active Carbon*; Marcel Dekker: New York, 1988.

(13) Lee, J.; Kim, J.; Hyeon, T. Recent Progress in the Synthesis of Porous Carbon Materials. *Adv. Mater.* **2006**, *18*, 2073−2094.

(14) Lu, A. H.; Schmidt, W.; Spliethoff, B.; Schüth, F. Synthesis of Ordered Mesoporous Carbon with Bimodal Pore System and High Pore Volume. *Adv. Mater.* **2003**, *15*, 1602−1606.
(15) Schmidt, L. D.; Dauenhauer, P. J. Chemical Engineering: Hybrid Routes to Biofuels. *Nature* **2007**, *447*, 914−915.
(16) Titirici, M.-M.; Antonietti, M. Chemistry and Materials Options of Sustainable Carbon Materials Made by Hydrothermal Carbonization. *Chem. Soc. Rev.* **2010**, *39*, 103−116.
(17) Sun, X.; Li, Y. D. Colloidal Carbon Spheres and Their Core/Shell Structures with Noble-Metal Nanoparticles. *Angew. Chem., Int. Ed.* **2004**, *43*, 597−601.
(18) Sevilla, M.; Fuertesa, A. B.; Mokaya, R. High Density Hydrogen Storage in Superactivated Carbons from Hydrothermally Carbonized Renewable Organic Materials. *Energy Environ. Sci.* **2011**, *4*, 1400−1410.
(19) Fellinger, T.-P.; White, R.; Titirici, M.-M.; Antonietti, M. Borax-Mediated Formation of Carbon Aerogels from Glucose. *Adv. Funct. Mater.* **2012**, *22*, 3254−3260.
(20) Falco, C.; Sevilla, M.; White, R. J.; Rothe, R.; Titirici, M.-M. Renewable Nitrogen-Doped Hydrothermal Carbons Derived from Microalgae. *ChemSusChem* **2012**, *5*, 1834−1840.
(21) Zhang, P. F.; Yuan, J. Y.; Fellinger, T.-P.; Antonietti, M.; Li, H. R.; Wang, Y. Improving Hydrothermal Carbonization by Poly(ionic liquid)s. *Angew. Chem., Int. Ed.* **2013**, *52*, 6028−6032.
(22) Zhang, P. F.; Gong, Y. T.; Li, H. R.; Chen, Z. R.; Wang, Y. Solvent-free Aerobic Oxidation of Hydrocarbons and Alcohols with Pd@N-doped Carbon from Glucose. *Nat. Commun.* **2013**, *4*, 1593.
(23) Wang, Y.; Li, H. R.; Wang, C. M.; Jiang, H. Ionic Liquids as Catalytic Green Solvents for Cracking Reactions. *Chem. Commun.* **2004**, 1938−1939.
(24) Zhang, P. F.; Gong, Y. T.; Lv, Y. Q.; Guo, Y.; Wang, Y.; Wang, C. M.; Li, H. R. Ionic Liquids with Metal Chelate Anions. *Chem. Commun.* **2012**, *48*, 2334−2336.
(25) Wang, Y.; Zhang, J.; Wang, X.; Antonietti, M.; Li, H. R. Boron- and Fluorine-Containing Mesoporous Carbon Nitride Polymers: Metal-Free Catalysts for Cyclohexane Oxidation. *Angew. Chem., Int. Ed.* **2010**, *49*, 3356−3359.
(26) Zhang, P. F.; Wang, C. M.; Chen, Z. R.; Li, H. R. Acetylacetone-metal Catalyst Modified by Pyridinium Salt Group Applied to the NHPI-catalyzed Oxidation of Cholesteryl Acetate. *Catal. Sci. Technol.* **2011**, *1*, 1133−1137.
(27) Wang, Y.; Wang, C.; Zhang, L.; Li, H. R. Difference for SO_2 and CO_2 in TGML Ionic Liquids: A Theoretical Investigation. *Phys. Chem. Chem. Phys.* **2008**, *10*, 5976−5982.
(28) Paraknowitsch, J. P.; Zhang, J.; Su, D. S.; Thomas, A.; Antonietti, M. Ionic Liquids as Precursors for Nitrogen-Doped Graphitic Carbon. *Adv. Mater.* **2010**, *22*, 87−92.
(29) Zhao, L.; Hu, Y. S.; Li, H.; Wang, Z. X.; Chen, L. Q. Porous $Li_4Ti_5O_{12}$ Coated with N-Doped Carbon from Ionic Liquids for Li-Ion Batteries. *Adv. Mater.* **2011**, *23*, 1385−1388.
(30) Plechkova, N. V.; Seddon, K. R. Applications of Ionic Liquids in the Chemical Industry. *Chem. Soc. Rev.* **2008**, *37*, 123−150.
(31) Rogers, R. D.; Seddon, K. R. Ionic Liquids-Solvents of the Future? *Science* **2003**, *302*, 792−793.
(32) Lee, J. S.; Wang, X. Q.; Luo, H. M.; Baker, G. A.; Dai, S. Facile Ionothermal Synthesis of Microporous and Mesoporous Carbons from Task Specific Ionic Liquids. *J. Am. Chem. Soc.* **2009**, *131*, 4596−4597.
(33) Lee, J. S.; Wang, X. Q.; Luo, H. M.; Dai, S. Fluidic Carbon Precursors for Formation of Functional Carbon under Ambient Pressure Based on Ionic Liquids. *Adv. Mater.* **2010**, *22*, 1004−1007.
(34) Fulvio, P.; Lee, J. S.; Mayes, R.; Wang, X.; Mahurina, S.; Dai, S. Boron and Nitrogen-rich Carbons from Ionic Liquid Precursors with Tailorable Surface Properties. *Phys. Chem. Chem. Phys.* **2011**, *13*, 13486−13491.
(35) Swatloski, R.; Spear, S.; Holbrey, J.; Rogers, R. D. Dissolution of Cellose with Ionic Liquids. *J. Am. Chem. Soc.* **2002**, *124*, 4974−4975.
(36) Wang, H.; Gurau, G.; Rogers, R. D. Ionic Liquid Processing of Cellulose. *Chem. Soc. Rev.* **2012**, *41*, 1519−1537.
(37) Turner, M. B.; Spear, S.; Holbrey, J.; Rogers, R. D. Production of Bioactive Cellulose Films Reconstituted from Ionic Liquids. *Biomacromolecules* **2004**, *5*, 1379−1384.
(38) Taubert, A.; Li, Z. Inorganic Materials from Ionic Liquids. *Dalton Trans.* **2007**, 723−727.
(39) Antonietti, M.; Kuang, D.; Smarsly, B.; Zhou, Y. Ionic Liquids for the Convenient Synthesis of Functional Nanoparticles and Other Inorganic Nanostructures. *Angew. Chem., Int. Ed.* **2004**, *43*, 4988−4992.
(40) Ma, Z.; Yu, J.; Dai, S. Preparation of Inorganic Materials using Ionic Liquids. *Adv. Mater.* **2010**, *22*, 261−285.
(41) Morris, R. E. Ionothermal Synthesis-Ionic Liquids as Functional Solvents in the Preparation of Crystalline Materials. *Chem. Commun.* **2009**, 2990−2998.
(42) Xie, Z.-L.; White, R. J.; Weber, J.; Taubert, A.; Titirici, M.-M. Hierarchical Porous Carbonaceous Materials via Ionothermal Carbonization of Carbohydrates. *J. Mater. Chem.* **2011**, *21*, 7434−7442.
(43) Bojdys, M. J.; Müller, J.-O.; Antonietti, M.; Thomas, A. Ionothermal Synthesis of Crystalline, Condensed, Graphitic Carbon Nitride. *Chem.—Eur. J.* **2008**, *14*, 8177−8182.
(44) Yu, L.; Falco, C.; Weber, J.; White, R.; Howe, J.; Titirici, M.-M. Carbohydrate-derived Hydrothermal Carbons: A Thorough Characterization Study. *Langmuir* **2012**, *28*, 12373−12383.
(45) Cooper, E. R.; Andrews, C. D.; Wheatley, P. S.; Webb, P. B.; Wormald, P.; Morris, R. E. Ionic Liquids and Eutectic Mixtures as Solvent and Template in Synthesis of Zeolite Analogues. *Nature* **2004**, *430*, 1012−1016.
(46) Sevilla, M.; Maciá-Agulló, J.; Fuertes, A. B. Hydrothermal Carbonization of Biomass as A Route for the Sequestration of CO_2: Chemical and Structural Properties of the Carbonized Products. *Biomass Bioenergy* **2011**, *35*, 3152−3159.
(47) Guilminot, E.; Gavillon, R.; Chatenet, M.; Berthon-Fabry, S.; Rigacci, A.; Budtova, T. New Nanostructured Carbons Based on Porous Cellulose: Elaboration, Pyrolysis and Use as Platinum Nanoparticles Substrate for Oxygen Reduction Electrocatalysis. *J. Power Sources* **2008**, *185*, 717−726.
(48) Zhu, H.; Yin, J.; Wang, X.; Wang, H.; Yang, X. R. Microorganism-Derived Heteroatom-Doped Carbon Materials for Oxygen Reduction and Supercapacitors. *Adv. Funct. Mater.* **2013**, *23*, 1305−1312.
(49) Antal, M. J.; Mok, W. S. L.; Richards, G. N. Mechanism of Formation of 5-(hydroxymethyl)-2-furaldehyde from d-Fructose and Sucrose. *Carbohydr. Res.* **1990**, *199*, 91−109.
(50) Wang, Y.; Li, H. R.; Han, S. J. Structure and Conformation Properties of 1-Alkyl-3-Methylimidazolium Halide Ionic Liquids: A Density-Functional Theory Study. *J. Chem. Phys.* **2005**, *123*, 174501.
(51) Wang, Y.; Li, H. R.; Han, S. J. The Chemical Nature of the +C-H···X^- (X = Cl or Br) Interaction in Imidazolium Halide Ionic Liquids. *J. Chem. Phys.* **2006**, *124*, 044504.
(52) Mele, A.; Tran, C. D.; Lacerda, S. H. D. The Structure of a Room-Temperature Ionic Liquid with and without Trace Amounts of Water: The Role of C-H···O and C-H···F Interactions in 1-*n*-Butyl-3-Methylimidazolium Tetrafluoroborate. *Angew. Chem., Int. Ed.* **2003**, *42*, 4364−4366.
(53) Zhang, P. F.; Yuan, J. Y.; Li, H. R.; Liu, X. F.; Xu, X.; Antonietti, M.; Wang, Y. Mesoporous Nitrogen-doped Carbon for Copper-mediated Ullmann-type C-O/-N/-S Cross-Coupling Reactions. *RSC Adv.* **2013**, *3*, 1890−1895.